



Optical properties and topography behavior in Cobalt Selenide nanostructure thin films under concentration changing

Scientific research paper

Dariussh Mehrparvar*, Nader Ghobadi

Department of physics, Faculty of sciences, Malayer University, Malayer, Iran

ARTICLE INFO

Article history:

Received 21 November 2020

Revised 31 May 2021

Accepted 12 April 2021

Available online 20 April 2021

Keywords:

Semiconductor nanoparticle films

Chemical bath deposition

Ions concentration

Surface topography

ABSTRACT

In this work, a simple solution synthesis route for CoSe nanostructure thin films using the chemical bath deposition method is presented. The ions concentration role that affects the evolution of the nanostructure thin film configuration and optical band gap in CoSe nanoparticle arrays are investigated. The experimental data showed that the ions concentration can affect the optical band gap, surface topography, and configuration of a thin layer in the same way as they affect the optical band gap and thin film thickness. Derivation ineffective thickness method has been employed for optical band gap determination and index transitions without any presumption about the transition nature. The useful numerical data for characterization of the surface topography extracted from atomic force microscopy data has been examined. The influence of the ions concentration on the 3-D surface morphology of cobalt selenide (CoSe) nanostructure thin films prepared by chemical bath deposition method has been considered.

1 Introduction

Quantum Confinement in nanostructured semiconductors is one of the most important characteristics that affect quantization when charge carriers are confined by small boundaries of quantum dots where the sizes of the confinement are less than the de Broglie wavelength of the charge carriers [1].

A suitable understanding of the process and preparation parameters controlling the deposition helps to modify the tailoring of the growth of nanoparticles to the favorable size and shape. The concentration of the constituent, one of the preparation parameters helps to alter the nanoparticle shape which has a determinative role in the procedure of the preparation [2].

Chemical solution deposition is one of the simplest and most economic procedures to grow stoichiometric CoSe

*Corresponding author.

Email address: dmehrpavar@malayeru.ac.ir

DOI: 10.22051/jitl.2021.33188.1046

thin films. It is comparatively low cost, easy to handle, suitable for large-area fabrication. In this procedure, the material is deposited onto a substrate from a supersaturated solution of aqueous precursors such as metal salts, complexing agents, and pH buffers. In other methods, the procedure of the preparation of the selenium is associated with many problems because its melting point is low [3].

Thin layers in the nanostructure form can be suitably considered using quantitative descriptions. In this regard, determining the three dimensional (3-D) surface topography is vital to approve the quality of thin film surfaces. Surface behavior is often complicated, they may be isotropic, or anisotropic or follow the Gaussian or non-Gaussian function. On the other hand, although the root mean square (RMS) roughness parameter provides statistics about the 3-D surface topography, it doesn't make any difference between peaks and valleys. In this framework, statistics of the surface topography has been mainly used for the characterization of the 3D engineering surface [4-7].

Derivation of ineffective thickness method (DITM) is presented to extract the optical band gap energy and the type of optical transitions in nanostructured semiconductors; firstly it shows an optical band gap independent of the measured thickness which only requires the measurement of the absorbance spectrum of the product. In this procedure, starting from the ineffective thickness method (ITM) procedure and by the first derivation of the absorbance data, the optical band gap and then the type of optical transition can be determined without any presumption about the type of transition [8, 9].

2 Model and theory

In this work, CoSe nanoparticle thin films are arranged by chemical solution deposition procedure using chemical reagents obtained from commercial sources in analytical reagent (AR) grade. The deposition steps include the following:

The CoSe thin films were grown on ordinary glass slides (26mm×7.6mm×2mm). Before deposition the substrates were washed in detergent, rinsed in acetone, ultrasonically cleaned and finally rinsed again with a mixture of double distilled water and methanol. The substrates were kept in vacuum. A 50 ml of 0.2M

($Co(CH_3COO)_2$) (to provide Co^{2+} ions) was taken in a glass beaker of 100 ml capacity, under constant stirring, before 25% ammonia was added slowly to this solution. At first the solution became light brown where by further addition of excess ammonia the solution became dark blue and transparent. 50 ml of freshly prepared 0.1M Na_2SeSO_3 was added slowly to the solution.

The glass substrates were vertically immersed in to the deposition solution, at the end of preparation process all the deposited substrates were removed from the chemical bath at suitable intervals (1-24 hours). Details of the deposition step are presented. The thickness of the deposited film was measured with the help of sensitive microbalance using the relation, $t = \frac{m}{\rho A}$ where, m is the mass of the deposited film, A is the area of the deposited film, and ρ is the density of the deposited material ($CoSe = 7.65 \text{ g/cm}^3$) in the bulk form [10].

3 Results and Discussion

3.1 XRD patterns

The XRD pattern helps researchers to find structural phase and space group of the related materials. Figure 1 shows the XRD pattern of the CoSe nanostructured thin films which indicate that these samples are pure-phase compounds. The product has peaks corresponding to the hexagonal CoSe (space group: P63/mmc) phase with cell constants $a = b = 0.363$ and $c = 0.530 \text{ nm}$, which are in agreement with JCPDS 00-015-0464. The intense and sharp diffraction peaks suggest that the obtained product is not well crystallized. The phase and crystalline structure of samples were determined by powder X-ray diffraction. XRD patterns were recorded by (Unisantis- XMD- 300, $CuK\alpha$, India) diffractometer using $CuK\alpha$ radiation ($\lambda = 1.5406 \text{ \AA}$) from $2\theta = 10^\circ$ to 80° .

3.2 Optical absorption

It is well known that if the particle size decreases the optical bandgap energy will increase. The optical absorption spectroscopy for band gap energy determination is the most popularly applied technique in exploring the quantum confinement effects in nanostructure semiconductors. The absorption data were analyzed using the following well known relation for near edge optical absorption of semiconductors

$$\alpha = K(h\nu - E_g)^m/h\nu, \quad (1)$$

where α is the absorption coefficient, $h\nu$ is the photon energy, K is a constant, E_g is the optical gap, m is a constant equal to 1/2 for direct bandgap semiconductors, and 2 for indirect gap semiconductors [11].

The spectral absorption was determined using a double beam UV-visible spectrometer (Model: Agilent Technologies, Cary series UV-Vis Spectrophotometer, Cary 100 UV-Vis) within the wavelength ranging from 190-900 nm.

3.3 Derivation Ineffective Thickness Method (DITM)

In the following section, derivation ineffective thickness method is employed for bandgap determination without thickness measurement. For bandgap energy determination of semiconductors, the authors usually use the Tauc model as of

$$\alpha(\nu)h\nu = C(h\nu - E_g)^m. \quad (2)$$

It is well known that $\alpha(\nu) = \frac{2.303 \times A(\lambda)}{d}$ based on Beer-Lamberts law. By Beer-Lamberts law we have

$$\left(\frac{2.303 \times A(\lambda)}{d} h\nu\right)^{1/m} = C(h\nu - E_g), \quad (3)$$

$$\left(\frac{2.303}{d}\right)^{1/m} (A(\lambda)h\nu)^{1/m} = C(h\nu - E_g), \quad (4)$$

in which $\left(\frac{2.303}{d}\right)^{1/m}$ is a constant number. We write

$$(A(\lambda)h\nu)^{1/m} = \frac{C}{\left(\frac{2.303}{d}\right)^{1/m}} (h\nu - E_g), \quad (5)$$

in which $k = \frac{C}{\left(\frac{2.303}{d}\right)^{1/m}}$ is another constant

$$A(\nu)E(\text{eV}) = K(E - E_g)^m, \quad (6)$$

$$A(\nu)h\nu = K(h\nu - E_g)^m. \quad (7)$$

Equation (7) is a revisited form of the Tauc model named ineffective thickness method (ITM)

$$\text{Ln}(A(\nu)E) = \text{Ln}(K(E - E_g)^m), \quad (8)$$

$$\text{Ln}(A(\nu)E) = m\text{Ln}(K) + m\text{Ln}(E - E_g). \quad (9)$$

In the following, the derivation ineffective thickness method (DITM) is presented. Hence we have

$$\frac{d[\text{Ln}[A(\nu)E]]}{d(B)} = \frac{m}{E - E_g}. \quad (10)$$

If the graph of $\frac{d\{\text{Ln}[A(\nu)E]\}}{dE}$ is drawn according to E , there will be a discontinuity at $E = E_g$. Therefore, E_g is determined, in eV, directly without any transition presupposition.

Using the energy gap values extracted from the derivation ineffective thickness method [y], the m values can be acquired (see Eq. 10) so the values of m can be extracted from the slope of the linear part of $\text{Ln}[A(\nu)E(\text{eV})]$ versus $\text{Ln}[E - E_g]$ plots. Plots of $\text{Ln}[A(\nu)E(\text{eV})]$ versus $\text{Ln}[E - E_g]$ are shown in Fig. 2. This procedure helps researchers to determine the m values related to transitions to natural, in other words, transition type (direct or indirect bandgap) [12-14].

The absorption spectra of the prepared CoSe nanostructured thin films with different concentrations (0.15, 0.25, and 0.35M deposition at 50°C) are shown in Fig. 2. The absorbance plot shows a red shift with increasing the concentrations from 0.15, 0.25, and 0.35mol that is based on the fact that absorption spectra of quantum dots are in low wavelengths. The observed red shifts are most possibly due to increases in the nanoparticles size. Dependence of nanoparticle size on the concentration of the ions is governed by the reaction in solution and on the substrate as a heterogeneous site for nucleation. In other words, the growth of small particles through precipitation via primary and secondary nucleation in a supersaturated solution will be different in the solution and on the substrate.

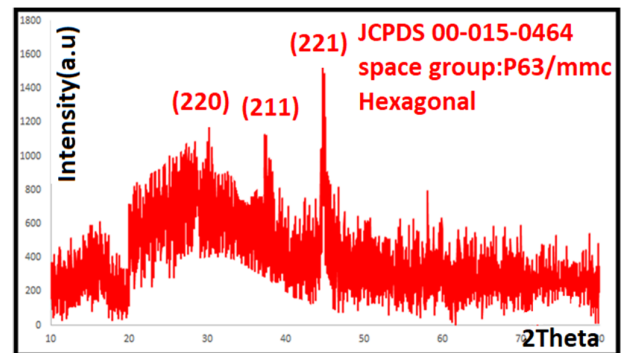


Figure 1. Representative XRD pattern of a sample with 0.35 mol at 50°C at 20 hours deposition time.

Archive of SID

To determine the optical band gap, two methods have been utilized, the Tauc model and DITM. For the Tauc model, the plot of $(Ah\nu)^2$ versus $(h\nu)$ is drawn in Fig 2. For CoSe thin films the best linear fit was obtained for $n = 1/2$ with various deposition concentrations. There is a difference between the two models where DITM determines optical bandgap without any presumption while Tauc model assumes that the transition is direct and the n index is equal to $1/2$. It seems that DITM is real and closer to the fact. The values of m index extracted from $\ln[A(\nu)E(\text{eV})]$ versus $\ln[E - E_g]$ are 0.306, 0.766, and 0.559 that show transitions are direct and closer to $1/2$ which means that this assumption is correct.

3.4 Characterization of the CoSe nanostructured thin films by atomic force microscopy (AFM)

The representation of the surface topography of the three nanostructured thin layers has been performed by an atomic force microscope using scan rates of 10–20 $\mu\text{m/s}$. All images were obtained over square areas of $1.0 \mu\text{m} \times 1.0 \mu\text{m}$. Data related to atomic force microscopy are the root mean square (RMS) roughness parameter and the power spectral density (PSD) function. Fractals are more suitable for providing information about the 3-D surface topography regarding difference between peaks and valleys. Determining the three dimensional (3-D) surface data is crucial to control the quality of thin films to engineering the surface behavior for improved optical and electrical properties. Experimental data extracted from the surface description of the AFM images (according to with ISO 25178-2: 2012) for the three samples with different ions concentration as root-mean-square deviation (S_q), skewness of topography height distribution (S_{sk}), kurtosis of topography height distribution (S_{ku}) and inclination angles determined from the AFM images are presented in Fig.3. $S_{sk} > 0$ for all samples, it shows the dominance of peaks on their surface, and the highest value is associated with the sample of 0.25 mol concentration (1.47). (S_q) for the sample with 0.25 mol has an optimal condition about 18.9 nm [9].

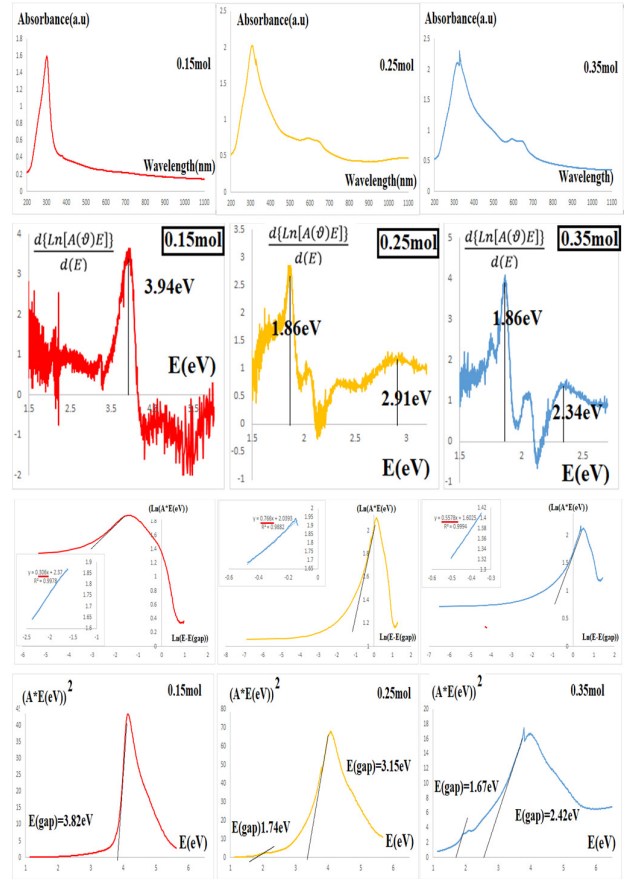


Figure 2. Plots of the optical properties for samples with 0.15, 0.25 mol at 50°C at 20hours deposition times.

Table 1: Root mean square deviation (S_q), skewness of topography height distribution (S_{sk}), kurtosis of topography height distribution (S_{ku}), S_p peak height, S_v valleys height determined from the AFM images.

| The basic properties of the height values distribution of the surface samples | S1 | S2 | S3 |
|---|---------|---------|---------|
| | 0.15mol | 0.25mol | 0.35mol |
| Rms (S_q) (nm) | 21.7 | 18.9 | 134 |
| Skew (S_{sk}) (nm) | 1.3 | 1.5 | 0.9 |
| Kurtosis (S_{ku}) (nm) | 4.3 | 4.9 | 2.1 |
| S_p (nm) | 80.6 | 74.4 | 305.0 |
| S_v (nm) | 28.4 | 20.6 | 119.0 |
| S_z (nm) | 109.0 | 95.0 | 424.0 |
| S_a (nm) | 17.7 | 15.2 | 118.0 |

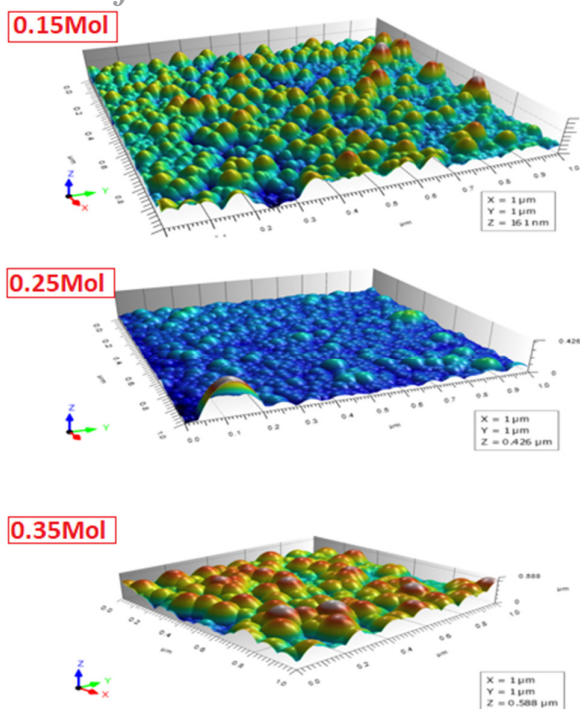


Figure 3. AFM images of the samples with 0.15, 0.25 and 0.35 mol and deposition time of 20 hours.

4 Conclusions

In summary, cobalt selenide nanostructured thin layers were successfully prepared at optimal temperature by chemical solution deposition on glass substrates. X-ray diffraction (XRD) confirms the hexagonal phase. The challenge between Tauc model and derivation ineffective thickness method is investigated. The DITM determines the real value rather than Tauc model without any presumption about transition to natural and thickness measurement. The values of transition index are extracted from $\ln [A(\nu)E(\text{eV})]$ versus $\ln [E - E_g]$. The remarkable role of the ions concentration on the 3-D surface morphology of cobalt selenide nanostructure thin films prepared by chemical bath deposition method has been considered. The ions concentration turned to the effect that the nanostructured semiconductors had the band gaps of around 1.8 eV and they could therefore be used for the quantum dot solar cell.

References

- [1] L.E. Brus, "Quantum crystallites and nonlinear optics." *Applied Physics A*, **53** (1991) 465.
- [2] C. Burda, X. Chen, R. Narayanan, M.A. El-Sayed, "Chemistry and Properties of Nanocrystals of Different Shapes." *Chemicals Reviews*, **105** (2005) 1025.
- [3] R.S. Mane, C.D. Lokhande, "Chemical deposition method for metal chalcogenide thin films." *Materials Chemistry and Physics*, **65** (2000) 1.
- [4] Ş. Tãlu, S. Stach, V. Sueiras, N. M. Ziebarth, "Fractal Analysis of AFM Images of the Surface of Bowman's Membrane of the Human Cornea." *Annals of biomedical engineering*, **43** (2015) 906.
- [5] S. Kulesza, M. Bramowicz, "A comparative study of correlation methods for determination of fractal parameters in surface characterization." *Applied Surface Science*, **293** (2014) 196.
- [6] A. Arman, T. Ghodselahi, M. Molamohammadi et al., "Microstructure and optical properties of Cu@Ni nanoparticles embedded in a-C:H." *Protection of Metals and Physical Chemistry of Surfaces*, **51** (2015) 575.
- [7] A. Arman Ş. Tãlu, C. Luna et al., "Micromorphology characterization of copper thin films by AFM and fractal analysis", *Journal of Materials Science: Materials in Electronics*, **26** (2015) 9630–9639.
- [8] N. Ghobadi, "Derivation of ineffective thickness method for investigation of the exact behavior of the optical transitions in nanostructured thin films." *Journal of Materials Science: Materials in Electronics*, **27** (2015) 8951.
- [9] N. Ghobadi, M. Ganji, C. Luna, A. Arman, A.A. pourian, "Effects of substrate temperature on the properties of sputtered TiN thin films." *Journal of Materials Science: Materials in Electronics*, **27** (2016) 2800.
- [10] N. Ghobadi, F. Dousi, "Shape, size and configuration tuning in ZnSe nanostructure thin films through deposition temperature, pH controlling and deposition time." *Journal of the Iranian Chemical Society*, **12** (2015) 757.

[11] J. Tauc, A. Menth, "States in the gap." *Journal of Non-Crystalline Solids*, **8-10** (1972) 569.

[12] D. Souri, M. Sarfehjou, A. R. Khezripour, "The effect of ambient temperature on the optical properties and crystalline quality of ZnSe and ZnSe:Cu NCs grown by rapid microwave irradiation." *Journal of Materials Science: Materials in Electronics*, **29** (2018) 3411.

[13] D. Souri, Z. Emaeili Tahan, "A new method for the determination of optical band gap and the nature of optical transitions in semiconductors." *Applied Physics B*, **119** (2015) 273.

[14] V. Dalouji, P. Ebrahimi, N. Tanhaee, N. Beryani Nezafat, L. Dejam, Sh. Solaymani, "The optical properties of Aluminum-Doped Zinc Oxide films (AZO): new methods for estimating gap states." *Journal of Superconductivity and Novel Magnetism*, **32** (2019) 1319.